Received 23 September 2025; Accepted 4 November 2025
https://doi.org/10.48612/letters/2025-4-324-330
https://elibrary.ru/wtpqbw

Simulation of fracture along grain boundaries containing superstructures of segregations in Al-Mg and Al-Ni systems

L. E. Karkina†, I. N. Karkin

†lidiakarkina@gmail.com

Mikheev's Institute of Metal Physics, Ural Branch of Russian Academy of Sciences, Ekaterinburg 620108, Russia

Abstract: Using the MD/MC Metropolis scheme, the most probable fracture-surface (FS) structures formed on a cleavage plane were studied in simulations of Al-3 at.% Mg and Al-3 at.% Ni alloys containing symmetric Σ5{013}<100> and Σ5{012}<100> boundaries with superstructures of segregations. The effect of FS ordered structures on grain-boundary (GB) decohesion processes is currently not studied, although the effect of an individual impurity atom on the features of grain-boundary fracture has been studied in detail. The resulting FS structures were analyzed depending on the type of grain boundaries and impurity atoms. It has been shown that the formation of FS superstructures reduces the energy of decohesion in all cases. The decrease in cohesive strength is most noticeable in Al-Ni compared to Al-Mg. A microscopic mechanism of the segregation formation and related GB reconstruction in Al alloys was revealed. For the solutes that have a larger atomic size and accept electrons from the matrix (such as Mg), one can assume that the deformation contribution will be dominant. It can be assumed that during FS superstructure formation, a preferred position of Mg is determined by the extra volume at the cleavage planes and/or reduced number of nearest neighbors. As a result, FS superstructures for the Al-Mg alloy are close to GB structures. The presence of directional bonds, as for the Al-Ni alloy, significantly changes FS structures. For both types of Σ5 GBs, stepped FS superstructures form directly under the cleavage planes.

Keywords: grain boundaries, superstructures, fracture energy, computer simulation

Acknowledgements. *The work was carried out as part of the state assignment of the Ministry of Education and Science of the Russian Federation for IMP Uran Ru.*

1. Introduction

Grain boundary segregations have a significant impact on many phenomena in polycrystals, such as recrystallization, strength and ductility, solid solution decomposition, and the nucleation of new phases [1]. Although the problem of segregations on GBs has been attracting the attention of researchers for many years, the impact of segregations on the GB structure and its properties remains a subject of discussion. Grain boundary segregations have a significant impact on many phenomena in polycrystals, such as recrystallization, strength and ductility, solid solution decomposition, and the nucleation of new phases [1]. Although the problem of segregations on the GB has been attracting the attention of researchers for many years, the impact of segregations on the GB structure and its properties remains a subject of discussions. The role of GB segregation becomes especially important in ultrafine grained materials, where the fractions of GB and bulk atoms are comparable [2, 3]. In this case, the formation of segregations at GBs significantly changes the conditions of the phase equilibrium [4 – 6] and thermal stability of microstructure [7, 8]. Al-Mg and Al-Zn alloys give a bright example of the dramatic dependence of segregations on the chemistry of alloying elements. In particular, for an Al-Mg system it was observed that Mg atoms tend to form heterogeneous agglomerations at GBs [4, 9], and it results in extra-hardening. However, the nature of the observed peculiarities of segregation is still not exactly known.

Computer simulation methods, such as density functional theory, molecular dynamics, and others, are an important supplement to experimental observations of grain boundary segregation behavior. The results of atomistic modeling of impurity segregations on GBs allow one to identify important parameters related to GB characteristics (GB energy, structure, and excess volume), as well as to the characteristics of the impurity atom (solution enthalpy, ionic radius).

New important information has been obtained in recent years using the hybrid simulation in MD/MC approach [14 – 16]. We used the Metropolis scheme [16], which at each MC step additionally included MD relaxation of the crystallite with a solute atom in a new trial position, and the probability of an atomic jump was determined taking into account the energy change due to relaxation. Such step-by-step relaxation in MD/MC simulations plays a significant role in correct description of the structural reconstruction of GBs in alloys with a close-packed fcc lattice, including Al-Mg and Al-Ni alloys. For alloys with a bcc lattice, MD relaxation

can be carried out through a larger number of MC steps. The occurrence of the GB structure (or highly ordered segregation superstructures in the classification of [14]) is controlled by several factors, including the crystallographic parameters of the GB, the characteristics of the dissolved or impurity atom, the energy associated with the distribution of the impurity atom near the GB sites, and others.

Grain boundary sliding and migration are processes that, along with intragranular sliding and accommodation processes at triple junctions, contribute to the plastic deformation of polycrystalline materials. The formation of ordered grain-boundary superstructures in weakly alloyed alloys and the local reconstruction of the region near the grain boundary significantly affect grain-boundary deformation. In [16–18], the processes of slip along grain boundaries in Al-Mg and Al-Ni alloys containing grain-boundary superstructures of impurity atoms were studied in detail. The effect of such ordered structures on the GB cohesion is currently unexplored, although the effect of a single impurity atom on the GB-localized fracture has been studied in detail (e. g., see [19–22] and the literature cited therein). In [22] it was noted that historically, authors of studies have reported embrittling potency as a single scalar value, assuming a single segregation site of importance at a GB and a particular cleavage plane. However, the topography of intergranular fracture surfaces is not generally known *a priori*. The authors of [22] proposed to consider the case, where many free surface permutations are systematically considered to model fracture of a GB.

In this work, the most probable FS structures formed on the cleavage plane during the simulation of GB cohesion in the Al-3 at.% Mg and Al-3 at.% Ni alloys containing symmetric Σ5 boundaries with GB superstructures were studied using the MD/MC procedure. The results obtained allowed us to establish that grain boundary superstructures in alloyed alloys change during crack opening and the formation of intergranular fracture surfaces, as well as to determine the effect of Mg and Ni on the GB cohesion in an Al bicrystal.

2. Simulation method

Atomistic modeling of the fracture process in Al-3 at.% Mg and Al-3 at.% Ni alloys was carried out in two stages. At the first stage, the well-tested rigid shift method without relaxation and with relaxation [18] was used. This method describes the effect of an impurity on intergranular embrittlement from an energy point of view. The "Griffith work" of brittle boundary separation (the fracture energy E_{frac}) is a linear function of the difference in binding energies for crystallites with GB and with free surfaces, referred to the boundary area. At the second stage, using the modified MD/MC Metropolis scheme [16], the most probable structures that form on the free surfaces of the opened crack were studied.

The energy E_{frac} was calculated for symmetric GBs Σ5{012}<100> and Σ5{013}<100> of special type with formed grain boundary superstructures. The grain boundaries with the lowest energy were selected for study [23]. When modeling the Al-Mg alloy, the MEAM potential by Lee et al [24] was used; for the Al-Ni alloy — EAM/alloy potential [25]. These potentials correctly describe many physical properties of both pure Al metal and Al-Ni and Al-Mg alloys. In particular, these potentials give energies of formation and interaction of point defects and their complexes, close to the results obtained in *ab initio* calculations [18]. These data are necessary input parameters for modeling the kinetics of precipitate formation in the alloy matrix. Numerical implementation was carried out using the LAMMPS package (Sandia National Laboratories) [26].

In all the cases, the YZ plane coincided with the GB plane, the OZ axis was parallel to the <100> tilt axis, and the OX direction was perpendicular to the GB plane. A crystallite contained two grains separated by a considered boundary located in its center. In all the cases, the size of grains along the OX direction perpendicular to the GB plane was ≈10 nm. In two mutually perpendicular directions OY and OZ, periodic boundary conditions were used in the GB plane. The period length along these directions was a multiple of the translation along the specified crystallographic direction. The values of translations along the <012>, <013>, and <100> directions are, respectively, $\sqrt{5}$A0, 1/2$\sqrt{10}$A0, and A0, where A0 is the lattice constant. In the course of modeling, a crystallite contained $(4–8)\times10^4$ atoms depending on the GB type. In the calculations the time step was 1.5 fs.

In [18], using combined MD/MC modeling at $T = 450$ K, which is typical in the experimental study of aging processes in aluminum alloys, was conducted. It was established that the interaction of various impurity atoms with grain boundaries Σ5{013}<100> and Σ5{012}<100> in Al matrix led to their structural reconstruction during segregation. It was shown that single-layer (Mg, Fig. 1a, b; Ni, Fig. 2c) and double-layer (Ni, Fig. 2a) segregations form. For GB Σ5{013}<100>, Mg atoms are located in the center of the structural units, Fig. 1a. The geometry of the boundaries in this case for the alloy and for Al coincides.

For the same GB, Ni atoms form a double layer near the GB (Fig. 2a), while the position of the GB shifts and the shape of the structural unit changes. Figure 1b shows the configuration of the region near GB Σ5{012}<100>, which also underwent structural reconstruction as a result of Mg atom segregation; a similar structure forms during Ni atom segregation (Fig. 2c). As discussed in [16], the nature of structural reconstruction of the GB is determined by the segregation energy of the impurity atom and its most energetically favorable position near the GB. For Ni for GB Σ5{013}<100>, there are two different sections (II and III), for which crack opening near the GB was considered (Fig. 2a, b). Sections I and III are equivalent.

During the formation of GB superstructures, the concentration of impurity atoms near the GB increases significantly. Naturally, the region near the GB is considered to be a part of the crystallite bounded by structural units. Then the average concentration of Mg atoms near the GB is 13.2 at.% and 16.7 at.%; Ni atoms — 24.2 at.% and 20.0 at.% for GBs Σ5{013} and Σ5{012}, respectively. The concentration of impurity atoms in the grain volume decreases to values below 1 at.%. At the second stage of the MD/MC Metropolis scheme, the exchange of Al atoms and impurity atoms was carried out within the region near the GB defined above. Destruction usually occurs at $T = 300$ K.

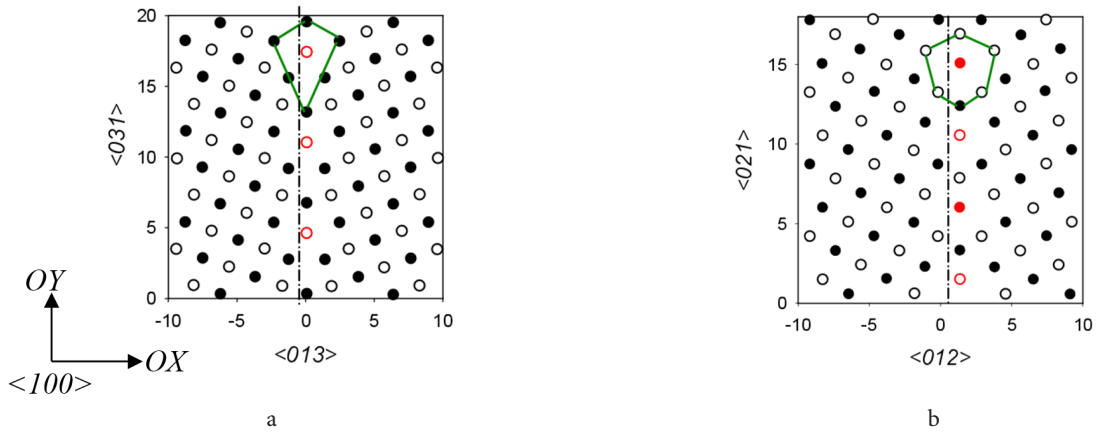

Fig. 1. (Color online) Fragment of a crystallite with a GB Σ5{013}<100> (a) and a GB Σ5{012}<100> (b) for Al-3 at.% Mg after 10^6 MD/MC relaxation steps [16]. Black and red circles represent Al atoms and Mg impurity atoms; open and shaded circles correspond to atoms in the nearest {100} planes. The coordinate axes are dimensioned in Å.Thin green lines highlight the structural units. The dashed line indicates the section perpendicular to which one part of the crystallite was shifted relative to the other during the formation of a crack.

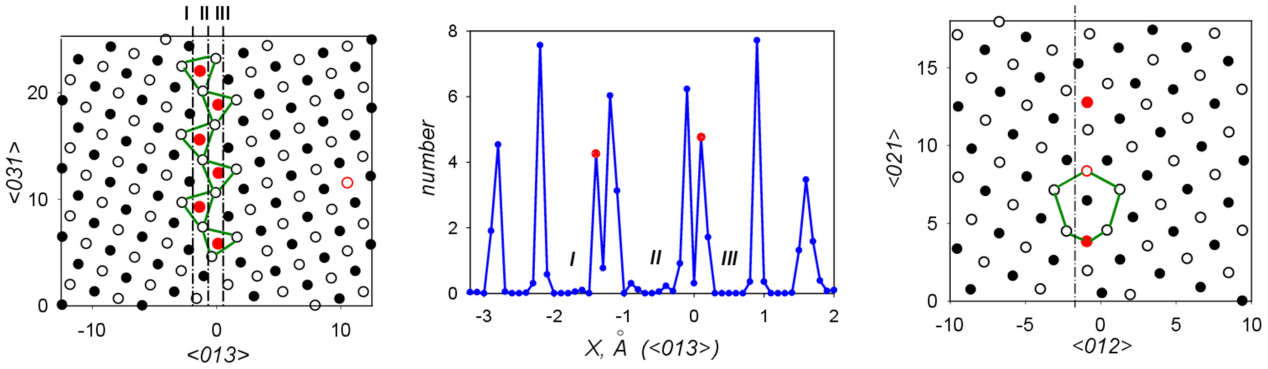

Fig. 2. (Color online) Fragment of a crystallite with the GB Σ5{013}<100> (a) and the GB Σ5{012}<100> (c) for Al-3 at.% Ni after 10^6 MD/MC relaxation steps [18].The distribution function of atoms along the *X* direction, perpendicular to the boundary plane near the GB Σ5{013}<100> (b). Other symbols are the same as in Fig. 1.

3. Simulation results

Figure 3 a presents the rigid and relaxed separation curves for the Al-3 at.% Mg alloy GB Σ5{013}. The curves are typical for all studied cases, but with significant quantitative differences; however, these issues will not be considered in the present work. We studied in detail the fracture energy E_{frac} (the region marked by a green ellipse in Fig. 3 a) and the change in intergranular fracture surfaces when comparing the non-relaxed and relaxed states of the surface and the formation of ordered surface configurations after conducting the MD/MC procedure.

Table 1 compares the fracture energy E_{frac} for all studied cases for Al-3 at.% Mg and Al-3 at.% Ni alloys. From Table 1, it can be seen that E_{frac} decreases by 9% to 17.5% upon surface restructuring and formation of a new surface superstructure after conducting the MD/MC procedure. For both types of GBs, the decrease in E_{frac} is more noticeable for the Al-3 at.% Ni alloy.

Figures 4 – 8 compare the configurations of fracture surface superstructures in the relaxed state and in the state relaxation + MD/MC. Figure 3 b shows the decrease in energy *dE* of the crystallite during the MD/MC procedure. The *dE* values reach saturation very quickly (in ~10^3 steps) compared to annealing time (in ~10^6 steps), so that the forming fracture surface structure can be considered equilibrium.

Table 1. Change in energy E_{frac} (J/m^2) upon crack opening in Al-3 at.% Mg and Al-3 at.% Ni alloys near symmetric GBs Σ5.

	Without relaxation	With relaxation	With relaxation + MD/MC
GB Σ5{013}<100>			
Al-Mg	1.52	1.34	1.22 (8.96%)
Al-Ni sec II	2.59	1.94	1.69 (12.9%)
Al-Ni sec III	2.65	2.02	1.68 (16.8%)
GB Σ5{012}<100>			
Al-Mg	1.71	1.57	1.41 (10.2%)
Al-Ni	2.56	2.11	1.74 (17.5%)

For Al-3 at.% Mg GB Σ5{013}<100> (Fig. 4), the addition of the MD/MC procedure does not significantly change the distribution of atoms on the figure plane. In the configuration after relaxation, Fig. 4 a, Al and Mg atoms are arranged in one chain (shown by arrow), as in the initial configuration (Fig. 1a). After completion of the MD/MC procedure, Fig. 4 b, the chain of Mg atoms is preserved, while Al atoms complete <110> chains of atoms in the matrix. Overall, the

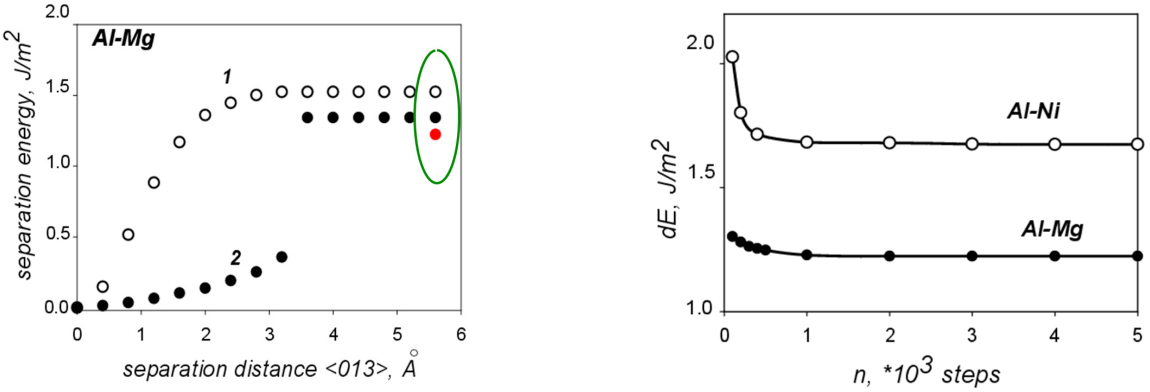

a b

Fig. 3. (Color online) Change in separation energy of Al-3 at.% Mg bicrystal at crack opening on GB Σ5{013}<100> (a). 1 — without relaxation, 2 — with relaxation. Red dot — the energy of decohesion after carrying out the MD/MC procedure for a crystallite with a free surface. Change in the energy of a bicrystal when carrying out the MD/MC procedure at $T = 300$ K in the Al-3 at.% Mg and Al-3 at.% Ni bicrystals (b).

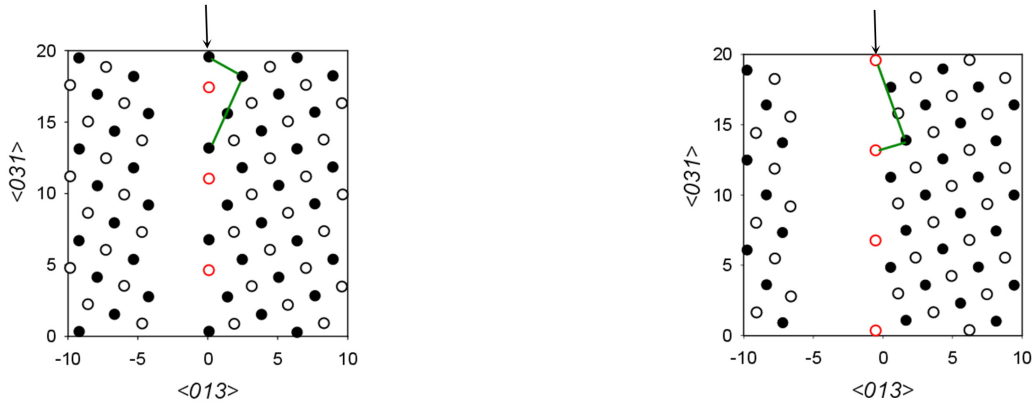

a b

Fig. 4. (Color online) Fragment of a crystallite Al-3 at.% Mg with a GB Σ5{013}<100> after fracture with relaxation (a) and with relaxation + MD/MC (b).

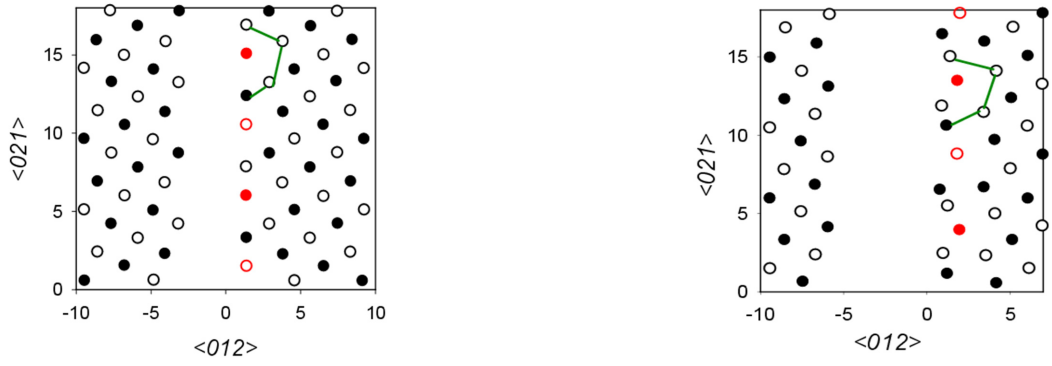

a b

Fig. 5. (Color online) Fragment of a crystallite Al-3 at.% Mg with a GB Σ5{012}<100> after fracture with relaxation (a) and with relaxation + MD/MC (b).

configuration of atoms on the surface forms a well-expressed stepped superstructure.

For Al-3 at.% Mg GB Σ5{012}<100> (Fig. 5), the addition of the MD/MC procedure changes the distribution of atoms on the figure plane. After completion of the MD/MC procedure, Fig. 5 b, the chain of Mg atoms is preserved, while Al atoms demonstrate significant restructuring. Fragments of the previous structural unit are preserved: the Mg atom is placed in the center of the new structural unit, but overall its configuration changes. An ordered superstructure forms near the free surface.

For Al-3 at.% Ni GB Σ5{013}<100> (section III), Fig. 6 a shows the non-relaxed configuration, where a fragment of the nanofaceted double-layer structure of Ni atoms is indicated. After relaxation (Fig. 6 b), the picture is generally preserved, but Ni impurity atoms shift by small distances: the distance between the two planes of Ni atoms decreases, impurity atoms also shift along the <031> direction, closing atomic rows of <110> type adjacent to the grain boundary from the grain body side. Conducting the additional MD/MC procedure significantly changes the pattern of Ni atom distribution near the free surface of the opened

crack (Fig. 6c), demonstrating the formation of a new superstructure. Ni atoms form a stepped structure located three atomic planes of Al away from the free surface. One of the Ni atom layers in the new superstructure repeats the position of atoms near the GB (shown by arrow in Fig. 6b, c), the remaining atoms form a repeating pattern with a shift of $a/2$ distance along the tilt axis <100>. The density of Ni atoms in the near-surface layer increases twofold compared to the initial grain boundary superstructure. Figure 6c shows the superstructure with completely filled positions, demonstrating the regular arrangement of Ni atoms in the fracture surface layer. For other sections along the <100> axis, the filling is not regular.

In section II (Fig. 7), near the surface, just as in Fig. 6, a stepped configuration is realized. Due to the lower concentration of Ni atoms on each of the free surfaces, such steps are formed fragmentarily (highlighted in green in Fig. 7b) along the GB plane, but their configuration is easily recognizable.

For the Al-3 at.% Ni alloy GB Σ5{012}, the formation of surface superstructure is shown in Fig. 8. From comparison of Fig. 8a and b, it can be seen that Ni atoms transition to

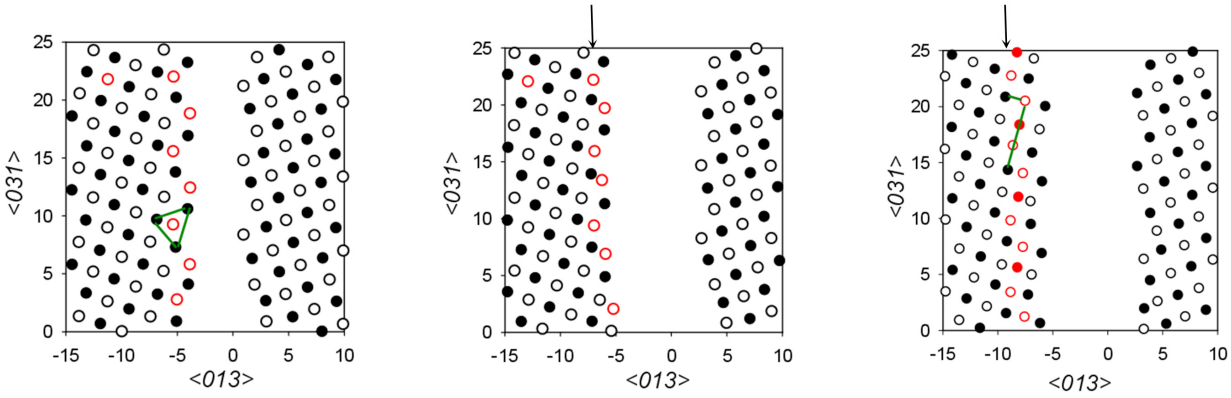

Fig. 6. (Color online) Fragment of a crystallite Al-3 at.% Ni with a GB Σ5{013}<100> after fracture (section III) without relaxation (a), with relaxation (b) and with relaxation + MD/MC (c).

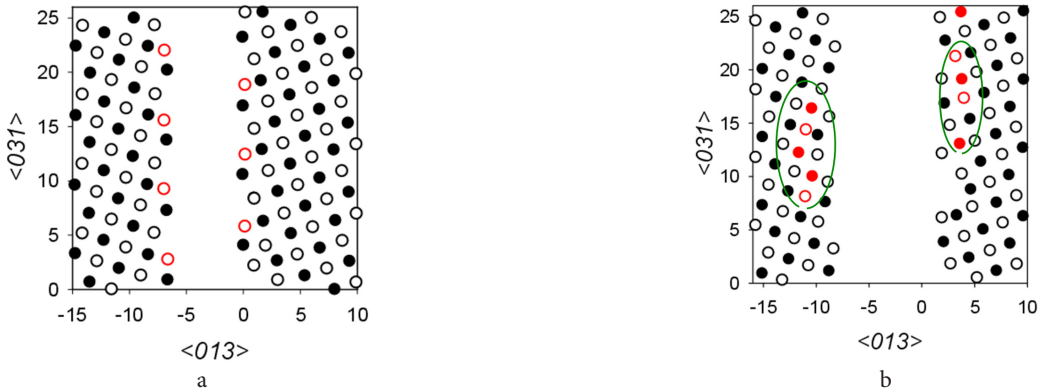

Fig. 7. (Color online) Fragment of a crystallite Al-3 at.% Ni with a GB Σ5{013}<100> after fracture (section II) without relaxation (a) and with relaxation + MD/MC (b).

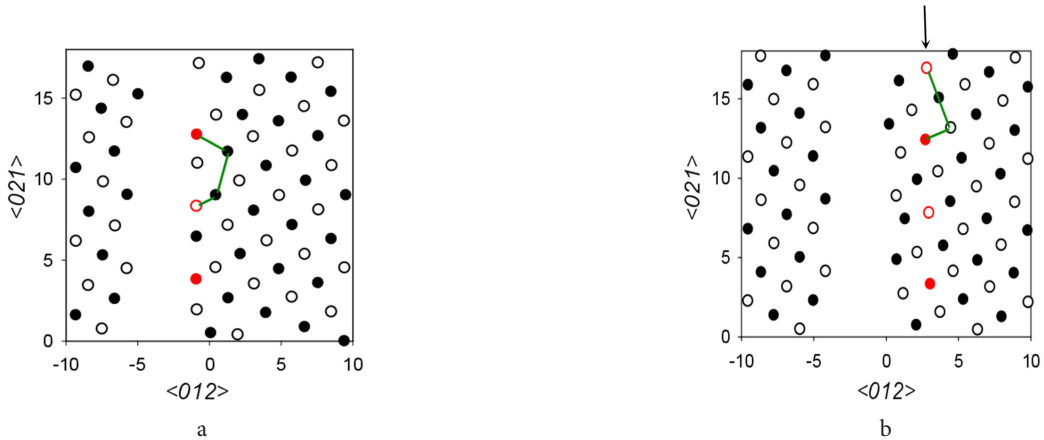

Fig. 8. (Color online) Fragment of a crystallite Al-3 at.% Ni with a GB Σ5{012}<100> after fracture without relaxation (a) and with relaxation + MD/MC (b).

several layers below the surface, forming a clearly visible stepped structure composed of Al and Ni atoms. Ni atoms on the figure plane lie along the <021> direction in a sequence close to the initial structure (shown by arrow in Fig. 8 b).

4. Discussion

The reconstruction of cleavage plane structure during simulation of GB cohesion in Al-3 at.% Mg and Al-3 at.% Ni alloys containing symmetric Σ5 boundaries with GB superstructures was studied. Comparison of energy during modeling of relaxed and relaxed + MD/MC states shows that relaxation alone cannot lead to the reconstruction of the surface layer and formation of a specific surface superstructure. The use of the modified MD/MC Metropolis scheme [16,17] assumes the possibility of fast diffusion in the near-surface layer. As shown in Fig. 3 b, the curves of energy change dE dependence on the number of MD/MC steps at $T = 300$ K reach a plateau very quickly (in ~10^3 steps), which demonstrates the possibility of using this method to describe diffusion-controlled reconstruction of the surface layer and obtaining equilibrium configuration.

In Table 1, it can be seen that all obtained surface superstructures correspond to more favorable energy E_{frac} compared to the energy of the relaxed structure. The change in fracture energy E_{frac} during reconstruction of cleavage planes for both types of GBs is more noticeable for the Al-3 at.% Ni alloy. The relative energy decrease upon FS superstructure formation for the AlMg alloy is (9–10)%, while for the AlNi alloy it is (13–17.5)%. In [16], using both MD/MC and *ab initio* methods, a microscopic mechanism of the segregation formation and related GB reconstruction in Al alloys was revealed. For the solutes that have a larger atomic size and accept electrons from the matrix (such as Mg), one can assume that the deformation contribution will be dominant. It can be assumed that during FS superstructure formation, a preferred position of Mg is determined by the extra volume at the cleavage planes and/or reduced number of nearest neighbors. As a result, FS superstructures for the Al-3 at.% Mg alloy are close to GB structures, Figs. 4 b and 5 b. The presence of directional bonds, as for the Al-3 at.% Ni alloy, significantly changes FS structures. For both types of Σ5 GBs, stepped FS superstructures form directly under the cleavage planes, Figs. 6 – 8.

5. Conclusions

Using the modified MD/MC Metropolis scheme, it was established that:

– in the Al-3 at.% Mg and Al-3 at.% Ni alloys that contain symmetric GBs Σ5{013} and Σ5{012}, ordered FS superstructures are formed during reconstruction of cleavage planes;

– the formation of FS structures leads to a decrease in the fracture energy, and to a greater extent for the Al-3 at.% Ni alloy as compared to the Al-3 at.% Mg alloy;

– FS structures for the Al-3 at.% Mg alloy are close to GB structures for this alloy, which is due to the extra volume at the cleavage planes and/or reduced number of the nearest neighbors;

– the presence of directional bonds for the Al-3 at.% Ni alloy significantly changes the FS structures. For both types of Σ5 GBs, the stepped FS superstructures are formed directly beneath the cleavage planes.

References

1. P. Lejček, Grain Boundary Segregation in Metals, Springer, Berlin, Germany, 2010, 249 p.
2. R. Z. Valiev, Nanostructuring of metals by severe plastic deformation for advanced properties. Nat. Mater. 3 (2004) 511–516.
3. X. Sauvage, G. Wilde, S. V. Divinski, Z. Horita, R. Z. Valiev, Grain boundaries in ultrafine in ultrafine grained materials processed by severe plastic deformation and related phenomena. Mater. Sci. Eng. A 540 (2012) 1–12.
4. P. P. Chatterjee, S. K. Pabi, I. Manna, An allotropic transformation induced by mechanical alloying. J. Appl. Phys. 86 (1999) 5912 – 5914.
5. M. Ben Makhlouf, T. Bachaga, J. J. Suñol, M. Mohamed Dammak, M. Khitouni, Synthesis and characterization of nanocrystalline Al-20 at% Cu powders produced by mechanical alloying. Metals 6 (2016) 145.
6. R. Kirchheim, Grain coarsening inhibited by solute segregation. Acta Mater. 50 (2002) 413 – 419.
7. J. R. Trelewicz, C. A. Schuh, Grain boundary segregation and thermodynamically stable binary nanocrystalline alloys. Phys. Rev. B 79 (2009) 094112.
8. T. Chookajorn, H. A. Murdoch, C. A. Schuh, Design of stable nanocrystalline alloys. Science 337 (2012) 951 – 954.
9. X. Sauvage, N. Enikeev, R. Valiev, Y. Nasedkina, M. Murashkin, Atomic-scale analysis of the segregation and precipitation mechanisms in a severely deformed Al-Mg alloy. Acta Mater. 72 (2014) 125 –136.
10. B. W. Krakauer, D. N. Seidman, Subnanometer scale study of segregation at grain boundaries in an Fe(Si) alloy. Acta Mater. 46 (1998) 6145 – 6161.
11. A. A. Salem, T. G. Langdon, T. R. McNelley, S. R. Kalidindi, Semiatin, S. L. Strain-path effects on the evolution of microstructure and texture during the severe-plastic deformation of aluminum. Metall. Mater. Trans. A 37 (2006) 2879 – 2891.
12. S. Zhang, O. Y. Kontsevoi, A. J. Freeman, G. B. Olson, Sodium-induced embrittlement of an aluminum grain boundary. Phys. Rev. B 82 (2010) 224107.
13. D. Scheiber, V. I. Razumovskiy, P. Puschnig, R. Pippan, L. Romaner, Ab initio description of segregation and cohesion of grain boundaries in W-25 at% Re alloys. Acta Mater. 88 (2015) 180 –189.
14. C. Hu, R. Dingreville, B. L. Boyce, Computational modeling of grain boundary segregation: A review, Comput. Mater. Sci. 232 (2024) 112596.
15. Z. Pan, T. J. Rupert, Effect of grain boundary character on segregation-induced structural transitions, Phys. Rev. B 93 (13) (2016) 134113.
16. L. Karkina, I. Karkin, A. Kuznetsov, Y. Gornostyrev, Alloying Element Segregation and Grain Boundary Reconstruction. Atomistic Modeling, Metals 9 (2019) 1319 –1331.
17. L. E. Kar'kina, I. N. Kar'kin, Yu. N. Gornostyrev, Effect of

Alloying Element Segregations on the Grain Boundary Sliding in Al-Mg and Al-Ni Alloy Bicrystals: Atomistic Modeling, Phys. Metals Metallog. 121 (2020) 817–822.
18. A. Kuznetsov, L. Karkina, Yu. Gornostyrev, P. Korzhavyi, Effects of Zn and Mg Segregations on the Grain Boundary Sliding and Cohesion in Al: Ab Initio Modeling, Metals 11 (2021) 631–641.
19. S. Zhang, O. Y. Kontsevoi, A. J. Freeman, G. B. Olson, First principles investigation of zinc-induced embrittlement in an aluminum grain boundary, Acta Materialia 59 (2011) 6155–6167.
20. V. I. Razumovskiy, A. V. Ruban, I. M. Razumovskii, A. Y. Lozovoi, V. N. Butrimb, Y. K. Vekilov, The effect of alloying elements on grain boundary and bulk cohesion in aluminum alloys: An ab initio study, Scr. Mater. 65 (2011) 926–929.
21. D. Zhao, O. M. Løvvik, K. Marthinsen, Y. Li, Segregation of Mg, Cu and their effects on the strength of Al Σ5 (210)[001] symmetrical tilt grain boundary, Acta Materialia 145 (2018) 235–246.
22. M. E. Fernandez, R. Dingreville, D. E. Spearot, Statistical perspective on embrittling potency for intergranular fracture, Phys. Rev. Mat. 6 (2022) 083602.
23. M. A. Tschopp, D. L. Macdowell, Asymmetric tilt grain boundary structure and energy in copper and aluminium, Philos. Mag. 87 (2007) 3871–3892.
24. Y.-M. Kim, N. J. Kim, B.-J. Lee, Atomistic Modeling of pure Mg and Mg-Al systems, Calphad 33 (2009) 650–657.
25. G. P. P. Pun, Y. Mishin, Development of an interatomic potential for the Ni-Al system, Philosophical Magazine 89 (2009) 3245–3267.
26. S. Plimpton, Fast Parallel Algorithms for Short-Range Molecular Dynamics, J. Comput. Phys. 117 (1) (1995) 1–19.